UM-P-81/18.

The Spectrum of ^{12}C in a Multi-Configuration Hartree-Fock Basis

K. Amos[A], I. Morrison[A], R. Smith[B] and K.W. Schmid[B,C]

A School of Physics, University of Melbourne, Parkville, Victoria.

B Research School of Physical Sciences, A.N.U., Canberra, A.C.T.

C Permanent Address: Institüt für Theoretische-Physik,
Universität Tübingen,
West Germany.

Abstract:

The energy level spectrum of ^{12}C is calculated in a truncated but large shell model space of projected one particle-one hole Hartree Fock determinants using a realistic G-matrix. Predictions of electromagnetic decays and electron scattering form factors are compared with experimental values.

1. Introduction

For many years the ^{12}C level spectrum has been a testing ground for theoretical models of nuclear structure ranging from the simplest T.D.A. through R.P.A. to sophisticated Shell model studies (Gillet and Vinh Mau 1964, Dehesa et al. 1977, Cohen and Kurath 1965, Amos and Morrison 1979). Following the success of the shell model calculations (Cohen and Kurath 1965) in reproducing most of the then available experimental data, it was assumed that there was little left to learn about the ^{12}C system. But analyses of more recent scattering experiments ((pp'), (π,π'), (ee') etc) and measurements of electromagnetic decay rates (Flanz et al. 1979, Amos and Morrison 1979, Love 1980, Thiessen 1980, Ajzenberg-Selove and Busch 1980) require a reevaluation either in terms of a refitted Op shell interaction or, as attempted herein, an ab-initio calculation. The latter was chosen in view of the ever increasing empirical information in the energy region above 12 MeV and therefore beyond the scope of the smaller basis, Op-shell models.

2. The PHM Model.

Within the framework of standard HF theory (Villars, 1963), an optimal reference determinantal wavefunction can be defined as

$$|\psi\rangle_A = \prod_{\alpha=1}^{A} b_\alpha^+ |-\rangle \qquad (1)$$

where the (axially symmetric) deformed single particle states $|\alpha\rangle$ can be expanded in terms of oscillator basis states. Thus, with

$$|\alpha\rangle = \sum_{\Omega} C_{nlj\ nlj,\alpha} |nlj\ \Omega\rangle \ , \qquad (2)$$

the coefficients, $C\alpha$, are solution of the Hartree Fock equations. The reference determinant and the complete set of lp-lh states (with respect to $|\psi\rangle_A$ and within the chosen oscillator basis) then define an intrinsic state basis for the PHM model (Schmid, 1980, 1981) from which the nuclear eigenstates are obtained by diagonalising the Hamiltonian of the system in a basis of physical states formed by angular momentum projection of these intrinsic states. This procedure limits spurious components in the resulting spectrum.

For $N \simeq Z$ nuclei, the physical state vectors will then have the form, using the standard projection operators

$\hat{P}(IMK)$ (McDonald, 1970),

$$|I^{\pi}MT;d\rangle = C^{I^{\pi}0}_{0d}\{\hat{P}(I^{+}M\ 0)|\rangle\}_{T=0}$$
$$+ \Sigma_{\beta L}C^{I^{\pi}T}_{\beta L;d}\{\hat{P}(IMK_{L\beta})\alpha^{\dagger}_{\beta}\alpha_{L}|\rangle\}_{T}\ , \qquad (3)$$

in which $\beta>F$ and $L\leq F$, the Fermi level. The eigenstates are then obtained (Watt, 1971) by solving the non-orthogonal eigenvalue problem

$$(H^{I\pi T}_{KK'} - E^{I\pi T}N^{I\pi T}_{KK'})C^{I^{\pi}T} = 0 \qquad (4)$$

in which the normalisation (overlap) matrix, N, measures the lack of orthogonality of the projected intrinsic state vectors The nuclear Hamiltonian, in standard form, is

$$H = \Sigma_{i=1}^{A} P_i^2/2m + \Sigma_{i<j}v_{ij}\ , \qquad (5)$$

in which the v_{ij} are the Barrett-Hewitt-McCarthy two nucleon g-matrices (Barrett, Hewitt and McCarthy, 1970, 1971). Centre of mass spuriosity in the eigenfunctions were minimised by a separate treatment of the centre of mass Hamiltonian.

Within the Os1/2 to Og9/2 inclusive spherical single particle basis (oscillator length = 1.79 fm.), the minimal determinant for ^{12}C was then obtained by using starting energies (ω) that well predict (in HF studies) the single

particle energies of ^{16}O and ^{40}Ca. By this means, the H.F. single particle spectrum, shown on the left in fig. 1, was obtained. Good agreement up to about 10 MeV with the (spherical), single particle spectrum used in recent R.P.A. calculations of ^{12}C (Dehesa et al., 1977) is apparent by inspection of the two relevant results in fig. 1. However, the underlying structure of the HF single particle states is contrary to the R.P.A. assumption of Op3/2 dominance as is evident in table 1 where the expansion coefficients of the HF states as defined by Eqn. (2) are given. Clearly while the Os1/2 and Op3/2 states dominate the expansions of the $\frac{1}{2}^+$ and $3/2^-|_1$ (k^π) states of the H.F. spectrum, the $\frac{1}{2}^-$ states are very strongly mixed. This is similar to Nilsson model calculations for oper shell nuclei (Irvine, 1972) and is largely independent of the character of the (realistic) g-matrices, in so far as it is a self consistent deformation field effect. Nevertheless some changes in the degree of mixing are caused by the specific character of the g-matrices i.e. different central, tensor and spin orbit components.

The degree of mixing determines the equivalent spherical single particle spectrum via

$$\langle e_i \rangle = \Sigma_\beta e_\beta A^2_{\beta i} \qquad (6)$$

and these are shown in the centre section of fig. 1. Clearly the effective (spherical) Op-shell splitting

is smaller (approximately 3 MeV) than used in usual calculations of spherical light nuclei (approximately 6 MeV for ^{16}O). The model thus will overestimate the $0p_{\frac{1}{2}}$ shell particle occupancy and this is revealed in table 2 where the occupancies are compared with those of a shell model (s.m.), an SU(3) (L.S coupling) limit model, and of the PHFBA model calculations (Smith, Morrison and Amos, 1980). Clearly the PHFBA and PHM occupancies are quite different to the shell model values with the PHM model being closest to the L-S limit. This is a measure of the effective spin-orbit splitting and has important consequences in electron scattering analyses (Amos and Morrison, 1979).

The PHM prediction of the ^{12}C energy spectrum is presented in Fig. 2 with the model energy levels being compared to the experimental values (Ajzenberg-Selove and Busch, 1980). (For convenience they have been grouped by parity and isospin). In making this comparison, we have not made any band head shift corrections (Schmid, 1980, 1981) and it should be noted that the low excitation scale has been compressed by 3 MeV, whence the comparison of the 2_1^+ energy values is not as severe as could be thought. Indeed the 2_1^+ T=0 state being too low by 1-1.5 MeV is quite common in such calculations (Caurier and Grammaticos, 1977). Of the positive parity isoscalar states, the 0_2^+ state at 7.65 MeV excitation (and possibly the next two as well) is known to be dominantly a quartet excitation (4p-4h) with respect to the deformed ^{12}C ground state. As such it

lies outside of our model configuration space and therefore has no obvious theoretical calculation partner in our spectrum, in contrast to the 1^+ and 4^+ states at 12.71 and 14.08 MeV excitation. Recent studies suggest other 1^+ isoscalar states in the region of 18 MeV excitation and of 2p-2h excitation. Mixtures of these excitations may be required to improve agreement between theoretical and experimental energies for the lowest $1^+(T=0)$ state.

Given the above consideration, globally the predicted spectrum is in good agreement with experiment especially since there are no free parameters in the interaction. In particular the parity and isospin band head energies are well predicted as are state sequences where empirical levels have been resolved.

We will be specifically interested hereafter with the 1^+ and 2^+ isovector states at 15.11 and 16.14 MeV excitations as these can be identified with wave functions of our PHM model; albeit that we predict other and nearly isovector 1^+ and 2^+ states. Such have not been seen empirically. Whilst no other states will be considered, we note the existence of a number of isoscalar and isovector 2^-, 3^- and 4^- states in the 17-20 MeV excitation region. Such may have been observed in recent electron and pion inelastic scattering studies (Thiessen, 1980). In view of the interest in such states in ^{16}O in the 18 MeV region vis-à-vis isospin mixing (Barker et al., 1981), further

study of such states (and reaction to them) in ^{12}C is planned.

From the calculated dipole states, the isoscalar and isovector E1 energy weighted sum rules were evaluated. The isoscalar component, which will vanish if the centre of mass spuriosity has been eliminated, was found to be only 2% of the isovector value.

3. Transition Rates.

Electromagnetic transition rates for the excitation of nuclei are predicted by evaluating reduced matrix elements of sums of one body operators, t(i), between multinucleon states. The appropriate transition probabilities can be deduced to have the form (Nesci and Amos, 1977)

$$B(XI;J_i \to J_f) = [(2I+1)(2J_i+1)]^{-1}$$

$$\{\Sigma_{j_1 j_2 \alpha} S^{(\alpha)}_{j_1 j_2} \langle \phi_{j_2} || t_\alpha(i) || \phi_{j_1} \rangle\}^2 , \qquad (7)$$

in which the spectroscopic amplitudes, defined by

$$S^{(\alpha)}_{j_1 j_2} = \langle J_f(T_f) || [a^+_{j_2} \times a_{j_1}]^I_{(\alpha)} || J_i(T_i) \rangle , \qquad (8)$$

contain all the multinucleon structure information relevant to the transition. The same spectroscopic amplitudes are required in analyses of hadron inelastic scattering exciting the nuclear target state $|J_f(T_f)\rangle$ from the (ground) state $|J_i(T_i)\rangle$. For electromagnetic excitations, the one body operators have radial forms of r^L nature so that the single particle reduced matrix elements do not vary to any great extent with choice of bound state potential model, provided at least one relevant single particle state is bound by an MeV or more. Thus variation in predictions of electromagnetic transition rates of low multipolarity should reflect dominantly

the differences in the multinucleon spectroscopies chosen to specify the spectroscopic amplitudes.

With a study of ^{12}C transitions in mind, it is useful to define the spectroscopic amplitudes for a closed shell $(p3/2)^8$ model. For the 1^+ transitions,

$$S^{(\alpha)}_{\frac{1}{2}\frac{3}{2}} = \left(\frac{3}{2}\right)^{\frac{1}{2}} \{\delta_{\alpha\frac{1}{2}} + (-)^T \delta_{\alpha\frac{1}{2}}\} \tag{9}$$

are the only possible spectroscopic amplitudes if the 1^+ states are pure particle hole states. The M1 transition probabilities are then given by

$$\begin{aligned} &B(M1;0^+ \rightarrow 1^+(T)\ ) \\ &= \tfrac{1}{2}[\langle\phi_{\frac{1}{2}}||M1(p)||\phi 3/2\rangle \\ &\quad + (-)^T\langle\phi_{\frac{1}{2}}||M1(n)||\phi 3/2\rangle]^2. \end{aligned} \tag{10}$$

Using the free particle g-factors, this leads to predictions of 0.092 μ_N^2 and 11.262 μ_N^2 (μ_N = nuclear magneton) for the isoscalar and isovector excitations respectively. The relevant experimental values are $(0.045\pm0.006)\mu_N^2$ and $(2.78\pm0.09)\mu_N^2$ (Ajzenberg-Selove and Busch, 1980). Using the same model for E2 transitions we find

$$\begin{aligned} B(E2;0^+ \rightarrow 2^+) &= \tfrac{1}{2}[e_p\langle\phi_{\frac{1}{2}}||E2(p)||\phi 3/2\rangle \\ &+ (-)^T e_n\langle\phi_{\frac{1}{2}}||E2(n)||\phi 3/2\rangle] \end{aligned} \tag{11}$$

from which, with bare charges, a value of 5.85^2 fm^4 results for

both the isovector and isoscalar transitions. Empirically the 4.44 MeV isoscalar transition has a value of (38.8±2.2) e^2fm^4 whilst that of the 16.11 MeV isovector transition is (10.80±0.6)e^2fm^4; values that can be obtained provided proton (neutron) effective charges of 1.58e (1.0e) are used. While such large and dissimilar polarization charges (0.58e and 1.0e) emphasise its limitations, this naive spectroscopic model provides base values in the j-j coupling limit against which the results of more complex spectroscopies may be compared.

The relevant spectroscopic amplitudes in more complex models are given in tables 3, 4 and 5. Proton (and neutron) spectroscopic amplitudes for the excitation of the isoscalar 2^+ (4.44 MeV) state in ^{12}C are listed in table 3 along with the results of an Op-shell model (S.M.) and the large basis projected Hartree-Fock (PHFBA) calculations (Amos and Morrison, 1979). In addition the relevant single particle reduced E2 matrix elements are given in column 4 from which the listed B(E2) values were obtained. Two factors emerge from this tabulation. First, while any non Op-Shell transition density is noticeably smaller than those within the Op-shell, their influence in B(E2), (ee') and (pp') predictions (Amos and Morrison, 1979) are significant. In such a 'collective' excitation all single particle contributions tend to add coherently. Such (isoscalar) B(E2) values are therefore insensitive to distribution of the Op-shell transition strengths through variations within the spectroscopic models. The

difference between the PHM and PHFBA results is primarily due to the destructive interference of the 0f-1p shell transition amplitudes in the PHM model. Nevertheless some physical attributes of the transition are sensitive to the relative contributions of the 0p shell transitions in particular. The electron scattering transverse form factor is one such property being, as it is, sensitive to spin-orbit effects in the nuclear states. In particular the magnetisation (spin current) contributions to transverse electric and magnetic form factors is maximised in the j-j limit and vanishes identically in the L-S (no spin orbit) limit. This sensitivity is evident in fig. 3 wherein the longitudinal and transverse form factors for the model calculations are compared with data (Flanz et al. 1978). Clearly the PHM model (solid lines) and PHFBA model (large dash lines) predictions are similar in form for both the longitudinal and transverse form factors, notbably in the peak momentum for the transverse form factor, since the shape variations reflect our use of different oscillator lengths. Clearly both HF based calculation results are distinct from the (small basis) shell model results for the transverse form factor. The shell model result for the longitudinal form factor, which includes a scaling correction for a polarization change of 0.5e, shows that an effective charge can account for any lack of coherence strength. This is not possible with the transverse form factor however since for momentum transfers greater than 1 fm^{-1} magnetisation effects dominate form factor calculations (whence the PHM results,

being nearest to the L-S limit, are poorest) whilst for low momentum transfer values, the convection currents dominate and hence the failure of the small basis shell model prediction. It appears, therefore, that a large basis HF calculation with the appropriate spin-orbit splitting may reproduce the data. The isospin and/or spin flip transitions, (specifically the $2_1^+(T=1)$, $1^+(T=0)$ and $1^+(T=4)$ states) are not 'collective' and are primarily determined by the $0\hbar\omega$ (0p-Shell) particle transitions. Such is clearly the case for the $2^+(T=1)$ transition when the PHM model spectroscopic amplitudes given in table 4 are considered. Further if the single particle elements, also given in table 4, are used to estimate the isovector B(E2) value, strong cancellations occur and predictions then are very sensitive to details of the spectroscopy. As a consequence, our PHM calculation gave a value of 0.02 e^2fm^4 for this isovector B(E2) value whilst the naive model yielded a value of $5.85e^2fm^4$; a value also predicted by an RPA calculation (Friebel et al., 1978). The suppression of transition strength is further displayed in fig. 4, wherein the predicted (PHM) longitudinal and transverse electric electron scattering form factors for excitation of the isovector 2^+ state are compared with data. Clearly the almost complete cancellation amongst 0p-shell contributions from the PHM spectroscopy persists in the low q form factors. The shell model calculations of Friebel et al. (Friebel et al., 1978) on the other hand gave quite good results.

The M1 excitation amplitues for the $1^+(T=0)$ and $1^+(T=1)$ and relevant single particle matrix elements (now different for protons and neutrons because of differing g-factors) are given in table 5 where the PHM results are compared with the 0p-shell model values. While it is evident that both transitions are dominated by the 0p-shell properties the different 0p 3/2 shell ground state occupancies (see table 2) give distinctly different values for the 1^+ spectroscopic amplitudes, and therefore for B(M1) predictions. The 0p-shell components of the PHM amplitudes by themselves lead to B(M1) values of 0.004 and 0.73 μ_N^2. For the isoscalar transition, it is the almost complete destructive interference between the op3/2→op1/2 and op1/2→op3/2 transitions that results in the small values, and while suppression of the isoscalar transition strength relative to the isovector is in accord with the experimental data, the suppression is too complete with the prediction being an order of magnitude below the experimental value (0.045 μ_N^2). Clearly the simple shell model result is much better, but even so it is still a factor of 3 weaker than experiment. Likewise for the isovector transition, strong cancellations yield too small a B(M1) value from the PHM model, specifically 0.77 μ_N^2 and which is to be compared to 0p-Shell model prediction of 2.77 μ_N^2 that agrees well with the experimental value of 2.78 μ_N^2. In both the isoscalar and isovector transition cases, recalling that the naive spectroscopic model yielded too large B(M1) values, model determinations of the magnetic dipole transition data are

very sensitive to the 0p-shell transition densities. Hadron scattering may also exhibit this sensitivity and the inability to date to fit data from the isoscalar excitation (Fox et al., 1979, Love, 1980) may still be a spectroscopic rather than a reaction dynamics problem.

The marked suppression of magnetic dipole transition strength as predicted by the PHM spectroscopy is evident in fig. 5 in which the isoscalar and isovector form factors are displayed. Whilst meson current corrections, for example, may significantly vary the larger q-value predictions, clearly the PHM calculations give too much cancellation between the relevant matrix elements. These results are far removed from the good fits obtained in a previous shell-model calculation (Flanz et al., 1979). However in that study, the isovector transition data was fitted by adjusting the spectroscopic amplitudes and thus, by allowing isospin mxing to occur between the two 1^+ states, the good fit to the 12.7 MeV state data resulted. Clearly the sensitivity of B(M1) values, and transverse form factors, to details of spectroscopy as we have demonstrated affords a good test of realistic (large basis) spectroscopic models of the ^{12}C system. In our present case, with the PHM approach, such tests reveal our inadequacy in the effective spherical Spin-orbit field strength.

4. Conclusion.

The PHM model has been successful in generating a quantitative representation of the spectrum of ^{12}C up to ≈ 20 MeV excitation, for those states which can be classified as predominanently 1p-1h, using a fully microscopic, parameter free, Hamiltonian consisting of a two nucleon G matrix and one nucleon kinetic energies only. Electron scattering data and B(M2) rates to a few selected levels, however, show that the G matrix underestimates the effective spin orbit splitting in the 0p shell. Due to the sensitivity of the spin-dependent data to small changes in the spin-orbit field, it should be possible to maintain the quality of the energy level spectrum whilst improving the electron-scattering predictions. An investigation using other G matrices is in progress.

References

Amos, K., and Morrison, I. (1979). Phys.Rev. C19, 2108.

Ajzenberg-Selove, F., and Busch, C.L. (1980). Nucl. Phys. A336, 1.

Barker, F., Smith, R., Morrison, I., and Amos, K. (1981). J. Phys. G (in press).

Barrett, B.R., Hewitt, R.G.L. and McCarthy, R.J. (1970). Phys.Rev. C2, 1199; ibid (1971). Phys.Rev. C3, 1137.

Caurier, E., and Grammaticos, B. (1977). Nucl.Phys. A279, 333.

Cohen, S. and Kurath, D. (1965). Nucl.Phys. 73, 1.

Dehesa, J.S., Krewald, S., Speth, J., and Faessler, A. (1977). Phys.Rev. C15, 1958.

Dehesa, J.S., Speth, J., and Faessler, A. (1977). Phys.Rev.Lett. 38, 208.

Flanz, J.B., Hicks, R.S., Lindgren, R.A., Peterson, G.A., Dubach, J. and Haxton, W.C. (1979). Phys.Rev.Letts. 43, 1922.

Friebel, A., Manakos, P., Richter, A., Spamer, E., Stock, W., and Titze, O. (1978). Nucl.Phys. A294, 129.

Fox, M., Morrison, I., Amos, K., and Weiss, I. (1979). Phys.Letts. 86B, 121.

Gillett, V. and Vinh Mau, N. (1964). Nucl.Phys. 54, 321.

Irvine, J. (1972) 'Nuclear Structure Theory', Permagon Press, Oxford, 1972.

Love, W.G. (1980). LAMPF Workshop on Nuclear Structure Studies with Intermediate Energy Probes, Los Alamos, New Mexico, USA.

MacDonald, N. (1970). Advances in Physics 19, 371.

Nesci, P., and Amos, K. (1977). Nucl.Phys. A284, 239.

Schmid, K.W. (1980). AN.FIS (Spain) 76, 63; (1981). Phys.Rev. (to be published).

Smith, R., Morrison, I., and Amos, K. (1980). Aust.J.Phys. 33, 1.

Thiessen, H.A. (1980) 'Proceedings of the 8th International Conference on High Energy Physics and Nuclear Structure'. Vancouver B.C. Ed. A. Thomas.

Villars, F. (1963). Proceedings of the International School of Physics "Enrico Fermi", Course XXIII (Academic Press, New York, 1963) p.1.

Watt, A. (1971). Nucl.Phys. A172, 260.

Table 1: H.F. single particle energies and wave functions in ^{12}C

k^{π}	ε[MeV]	0s1/2	1s1/2	0d3/2	0d5/2	0g9/2	
$1/2^+$	-36.76	.9751	.1349	.1206	-.1279	.0107	
$5/2^+$	- 3.65	-	-	-	.9977	-.0681	
$1/2^+$	- 1.98	-.0534	.8831	-.0657	.4584	-.0545	
$3/2^+$	- 1.31	-	-	.6733	.7355	-.0755	
$1/2^+$	4.60	.0907	-.3643	.5024	.7722	-.1020	
$3/2^+$	4.78	-	-	.7394	-.6687	.0784	
$1/2^+$	7.71	-.1952	.2632	.8537	-.4008	.0569	
$9/2^+$	21.53	-	-	-	-	1.0000	
$7/2^+$	23.24	-	-	-	-	1.0000	
$5/2^+$	24.46	-	-	-	.0681	.9977	
$3/2^+$	25.24	-	-	-.0073	.1086	.9941	
$1/2^+$	25.62	.0071	-.0055	-.0022	.1290	.9916	
		0p1/2	0p3/2	1p1/2	1p3/2	0p5/2	0p7/2
$3/2^-$	-17.64	-	.9845	-	.1128	.0801	-.0959
$7/2^-$	-16.48	.7222	.6701	.0796	.1061	-.0599	-.0901
$7/2^-$	- 3.57	.6710	-.7189	-.0040	.0243	-.1182	.1356
$7/2^-$	7.75	-	-	-	-	-	1.0000
$5/2^-$	9.85	-	-	-	-	.4592	.8883
$3/2^-$	10.21	-	.0709	-	-.8532	-.7537	-.4933
$7/2^-$	10.57	.0978	.0233	-.6233	-.6898	-.0980	-.3405
$3/2^-$	12.83	-	.1160	-	-.5067	.3056	.7978
$5/2^-$	13.65	-	-	-	-	.8883	-.4592
$7/2^-$	13.74	.0214	.1685	-.3919	-.0937	.1143	.8920
$3/2^-$	15.62	-	.1105	-	-.0148	-.9363	.3332
$7/2^-$	15.67	-.0100	.0498	.6534	-.6730	-.2461	.2388
$7/2^-$	16.36	-.1341	.0522	-.1569	.2250	-.9483	.0695

Table 2: Single particle occupancies in the ^{12}C ground state

j	S.M.	SU(3)	PHFBA	PHM
0s1	2.00	2.00	1.94	1.90
0p1	0.74	1.33	0.96	1.04
0p3	3.27	2.67	2.99	2.84
1s1	-	-	0.01	0.04
0d3	-	-	0.02	0.03
0d5	-	-	0.03	0.04
1p1	-	-	0.00	0.01
1p3	-	-	0.01	0.05
0f5	-	-	0.01	0.02
0f7	-	-	0.03	0.04

Table 3. Spectroscopic Amplitudes for the Excitation of the 2^+ T=0 (4.44 MeV) State in ^{12}C.

j_1	j_2	S.M.	PHFBA	PHM	E2 Element
0d3	0s1	-	0.114	0.170	2.65
0d5	0s1	-	0.128	0.184	3.24
0p3	0p1	1.195	1.086	0.935	3.42
1p3	0p1	-	0.054	0.141	-2.16
0f5	0p1	-	0.045	0.025	4.96
0p1	0p3	-0.704	-0.804	-0.845	-3.42
0p3	0p3	-0.503	-0.549	-0.654	-3.42
1p1	0p3	-	-	-0.095	2.16
1p3	0p3	-	-	-0.069	2.16
0f5	0p3	-	-	0.074	2.65
0f7	0p3	-	0.064	0.121	6.49
0d3	1s1	-	-	0.025	-4.33
0s1	0d3	-	-0.209	-0.203	-2.65
1s1	0d3	-	-	-0.028	-4.33
0s1	0d5	-	0.234	0.211	3.24
1s1	0d5	-	-	0.029	-5.30
0p3	1p1	-	-	0.097	-2.16
0p1	1p3	-	-	-0.131	2.16
0p3	1p3	-	-0.043	-0.055	2.16
0p1	0f5	-	0.056	0.101	4.96
0p3	0f5	-	-0.088	-0.108	-2.65
0p3	0f7	-	0.197	0.225	6.49
1p3	0f7	-	-	0.031	-8.21
B(E2)		13.5	33.9	26.0	

Table 4: Proton Spectroscopic Amplitudes for the Excitation of the 2^+ T=1 (16.11 MeV) State in ^{12}C

j_1	j_2	S	E2 Element
0p3	0p1	-0.393	3.42
1p3	0p1	-0.049	-2.16
0f5	0p1	-0.016	4.96
0p1	0p3	0.354	-3.42
0p3	0p3	-0.725	-3.42
1p1	0p3	-0.040	2.16
1p3	0p3	-0.093	2.16
0f5	0p3	-0.012	2.65
0s1	0d5	0.012	3.24
0p1	1p3	-0.014	2.16
0p3	1p3	0.033	2.16
0p1	0f5	-0.028	4.96
0p3	0f5	-0.039	-2.65
0p3	0f7	-0.015	6.49

Table 5: Proton Spectroscopic Amplitudes for ^{12}C $1^+(T)$ Excitations.

		T=0		T=1		Ml Elements	
j_1	j_2	S.M.	PHM	S.M.	PHM	P	n
0p1	0p1	0.053	0.066	0.071	0.128	0.32	0.76
0p3	0p1	-0.880	-0.644	-0.845	-0.578	2.59	-2.16
1p1	0p1	-	0.007	-	-0.014	-	-
1p3	0p1	-	-0.092	-	-0.084	-	-
0p1	0p3	-0.434	-0.461	-0.416	-0.490	-2.59	2.16
0p3	0p3	-0.017	-0.027	-0.093	-0.167	4.78	-2.41
1p1	0p3	-	-0.052	-	-0.055	-	-
1p3	0p3	-	-0.011	-	-0.032	-	-
0f5	0p3	-	0.003	-	0.011	-	-
0s1	1s1	-	0.023	-	0.016	-	-
0s1	0d3	-	0.136	-	-0.047	-	-
1s1	0d3	-	0.019	-	-0.006	-	-
0p1	1p1	-	0.060	-	-0.020	-	-
0p3	1p1	-	-0.010	-	-0.005	-	-
0p1	1p3	-	-0.026	-	0.025	-	-
0p3	1p3	-	0.008	-	0.031	-	-
0p3	0f5	-	0.081	-	-0.027	-	-
1p3	0f5	-	0.010	-	-0.004	-	-
0f7	0f5	-	-0.004	-	-0.011	4.15	-3.46
B(M1)		0.014	0.004	2.17	0.77		

Figure Captions

Fig. 1 The single particle spectrum associated with the Hartree Fock (H.F.) calculations (deformed field results classified by the k^{π} numbers shown to the left) compared to the equivalent spherical spectrum and the (spherical) R.P.A. spectrum identified by the labels on the right. The fermi levels are also shown.

Fig. 2 The ^{12}C energy spectrum resulting from the PHM calculations compared with the experimental values.

Fig. 3 The longitudinal and transverse (electric) form factors from inelastic electron scattering to the 2^{+}(T=0) 4.44 MeV state in ^{12}C. The solid lines give the PHM model predictions whilst the long and short dash lines are the predictions obtained using the PHFBA and Shell Model spectroscopy respectively (Amos and Morrison, 1979).

Fig. 4 The longitudinal (filled circles) and transverse (open circles) form factors, data and PHM predictions, for the isovector excitation by electron scattering of the 16.11 MeV 2^{+} state in ^{12}C.

Fig. 5 The transverse form factors, data and PHM predictions, for the magnetic dipole excitations in ^{12}C.

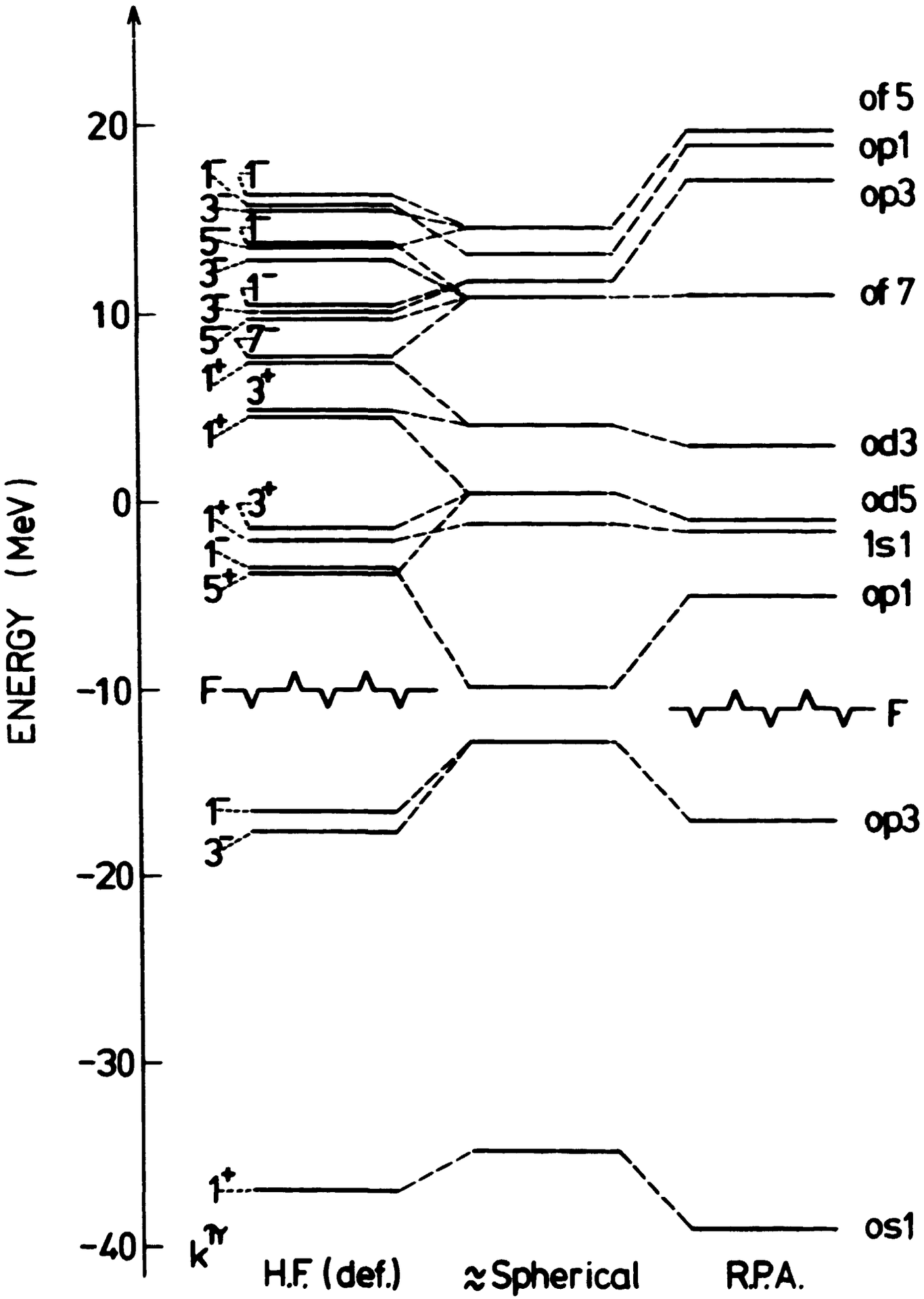
ENERGY (MeV)
20
10
0
-10
-20
-30
-40
of 5
op1
op3
of 7
od3
od5
1s1
op1
F
F
op3
os1
H.F. (def.)
≈Spherical
R.P.A.

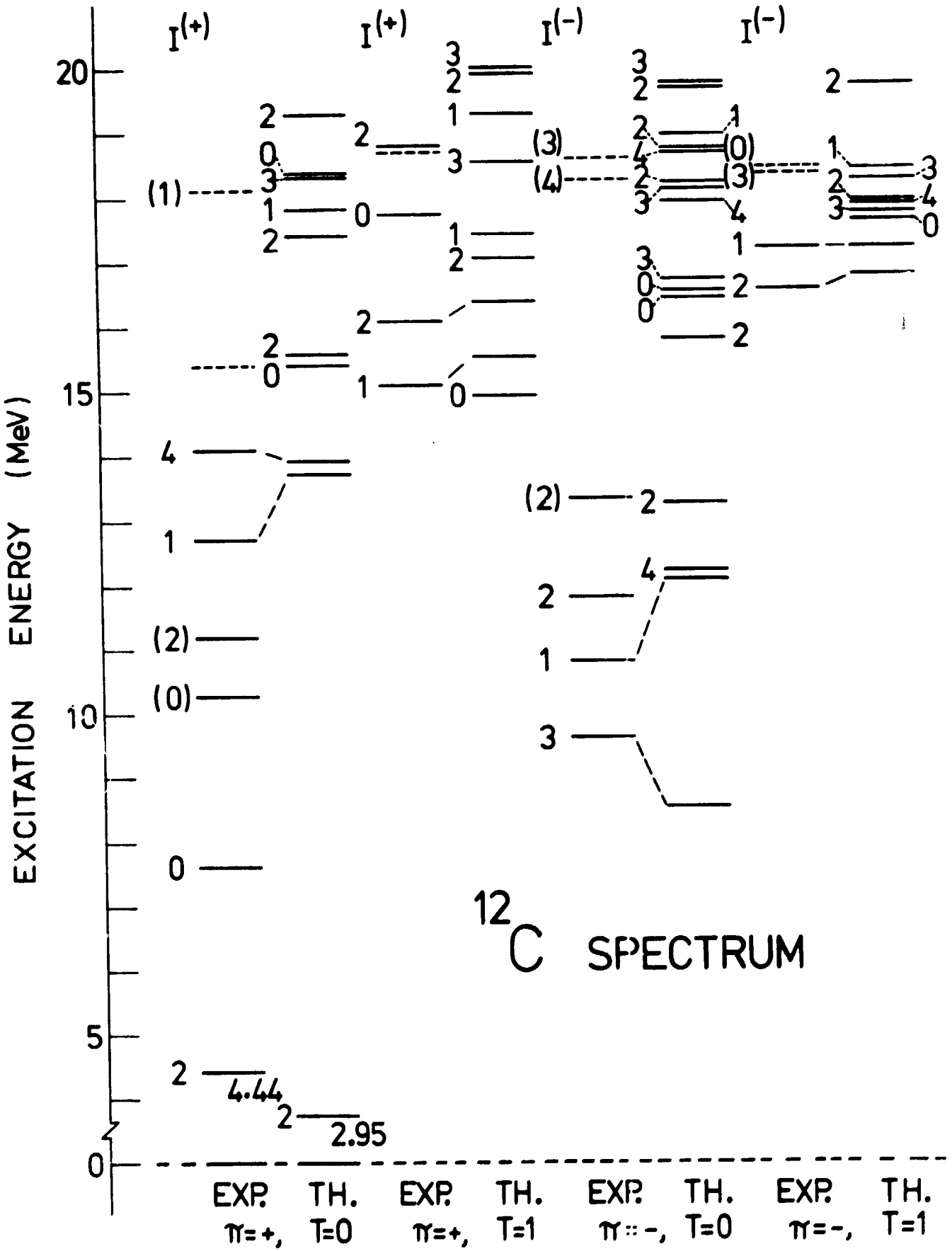
^{12}C SPECTRUM
EXCITATION ENERGY (MeV)
20
15
10
5
0
$I^{(+)}$
$I^{(+)}$
$I^{(-)}$
$I^{(-)}$
(1)
(2)
(0)
(3)
(4)
4.44
2.95
EXP. π=+, T=0
TH. π=+, T=0
EXP. π=+, T=1
TH. π=+, T=1
EXP. π=-, T=0
TH. π=-, T=0
EXP. π=-, T=1
TH. π=-, T=1

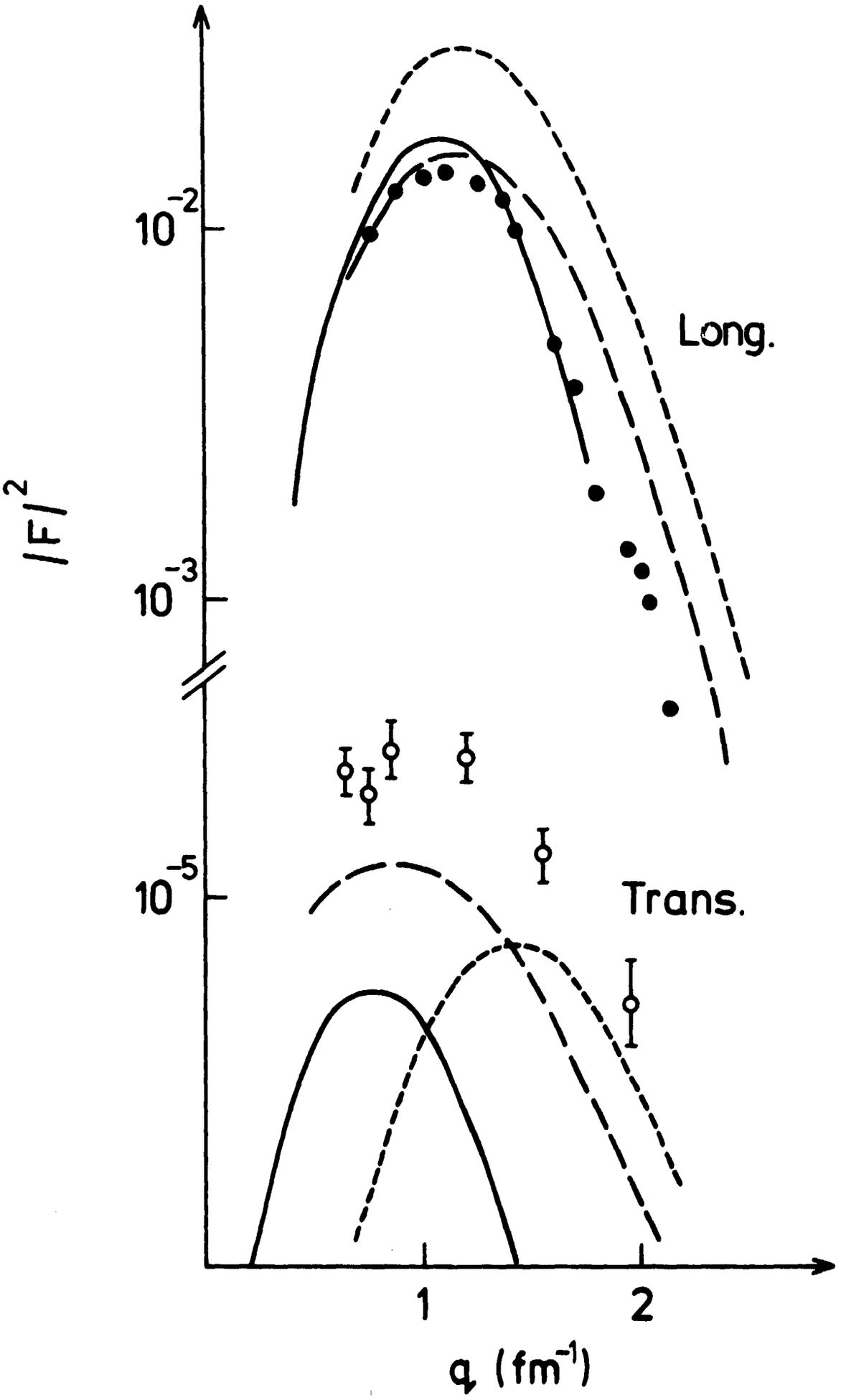
$|F|^2$
10^{-2}
10^{-3}
10^{-5}
Long.
Trans.
1
2
q (fm^{-1})

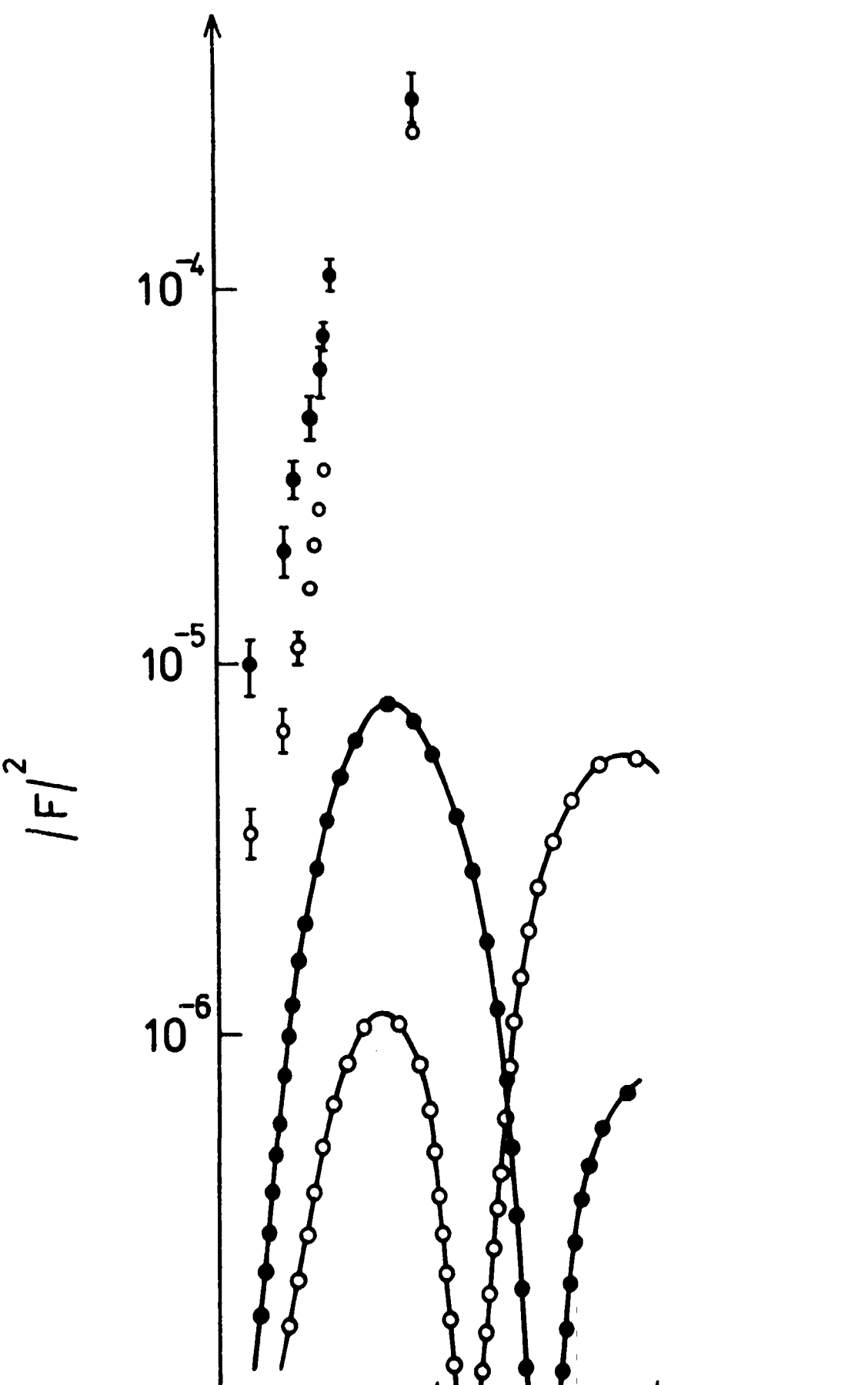
10^{-4}
10^{-5}
10^{-6}
$|F|^2$
1
2
q (fm^{-1})

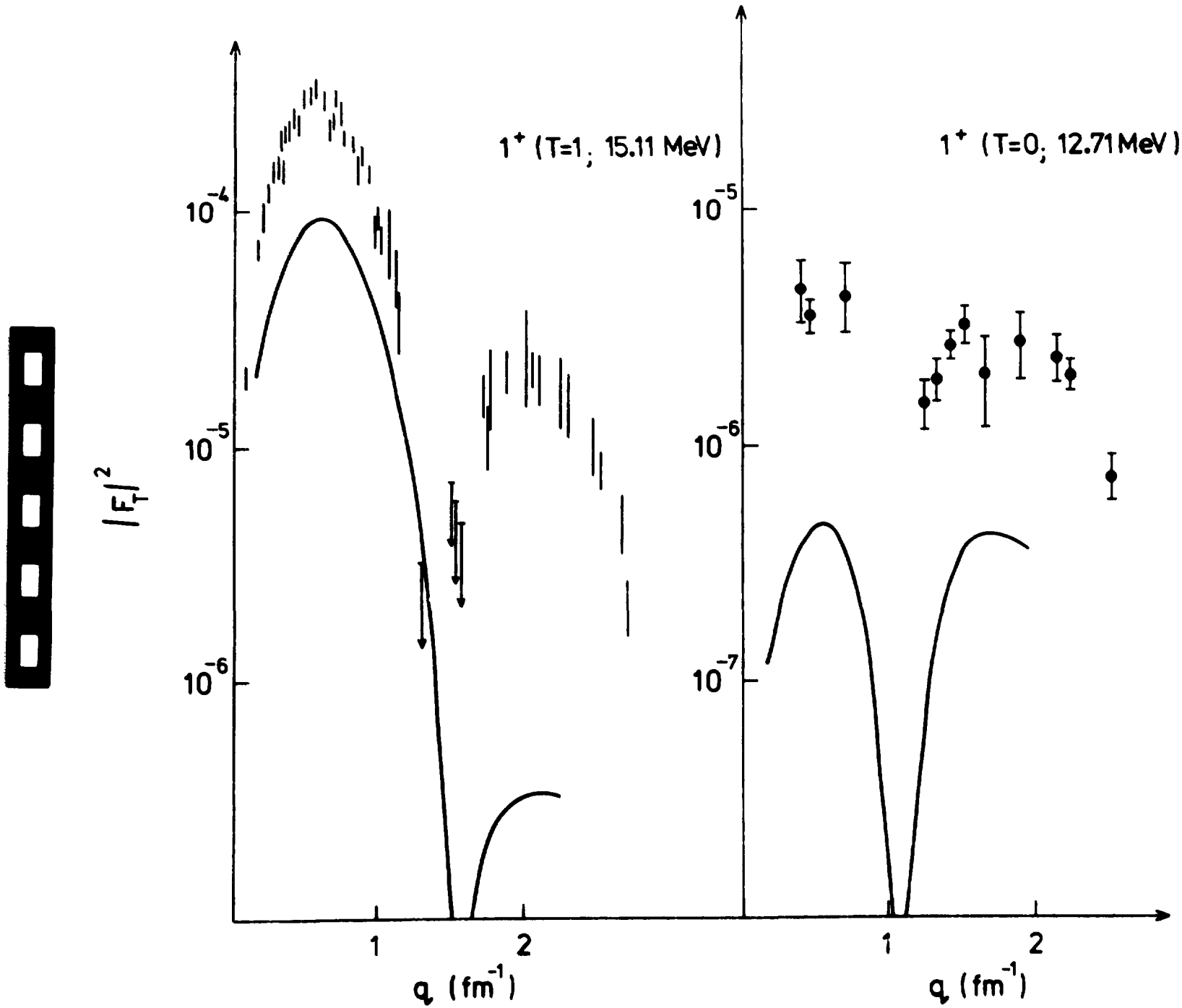
1+ (T=1; 15.11 MeV)
1+ (T=0; 12.71 MeV)
$|F_T|^2$
10^{-4}
10^{-5}
10^{-6}
10^{-5}
10^{-6}
10^{-7}
1
2
q (fm^{-1})
1
2
q (fm^{-1})